Lightning attachment processes of an "anomalous" triggered lightning discharge

D. Wang[1], W. R. Gamerota[2], M. A. Uman[2], N. Takagi[1], J. D. Hill[2], J. Pilkey[2], T. Ngin[2], D. M. Jordan[2], S. Mallick[2], and V. A. Rakov[2]

[1]Department of Electrical, Electronic and Computer Engineering, Gifu University, Gifu, Japan, [2]Department of Electrical and Computer Engineering, University of Florida, Gainesville, Florida, USA

Abstract Using a high-speed optical imaging system specifically designed for observing the lightning attachment process, we have documented the process for stepped, dart, and dart-stepped leaders in an anomalous rocket-triggered lightning flash that terminated on a 10 m grounded utility pole. The initiation of the first return stroke was found to occur at a height of 23 ± 3 m above the top of the utility pole and was associated with three "slow front" dE/dt pulses. A time of 1.5 μs later, a fast rise in luminosity at 18 ± 2 m was associated with a "fast transition" dE/dt pulse. The first return stroke propagated bidirectionally from its initiation height, as did subsequent return strokes from their initiation heights of 8 ± 1 m to 16 ± 2 m above the top of the utility pole. The initial upward speed of the first return stroke was 1.4×10^8 m/s, while its initial downward speed was 2.2×10^7 m/s. The channel bottom luminosity of the first return stroke rose more slowly to a two or more times larger amplitude than that of the subsequent stroke luminosities. In contrast, the National Lightning Detection Network-derived first-return-stroke peak current is smaller than that of the second and the third strokes, and our electric field records at 45 km show similar behavior for the initial field peaks of the first and subsequent strokes.

1. Introduction

A nine-stroke anomalous lightning flash was triggered at The International Center for Lightning Research and Testing (ICLRT) at Camp Blanding, Florida, on 15 May 2012 at 17:45:04.709106 (UT). That flash is described in detail by *Gamerota et al.* [2013]. An anomalous flash is a flash that is triggered by the classical (grounded wire) rocket-and-wire technique but in which the leaders do not follow the triggering wire remnants to ground, as is the case in the usual classical triggered lightning. Rather the anomalous leaders traverse a path through free space to ground, a path established by a downward stepped leader initiated from approximately the top of the triggering wire remnants some hundred meters above ground. When the downward stepped leader attaches to ground, a return stroke similar to the first return stroke in natural lightning occurs. Anomalous rocket-triggered lightning flashes provide a unique opportunity to study the characteristics of stepped leaders and first return strokes at very close range.

Using the Lightning Attachment Process Observation System (LAPOS) [*Wang et al.*, 2011, 2013], a high-speed optical system specifically designed for observing the lightning attachment process, we have documented the luminous properties of the anomalous lightning flash triggered at the ICLRT on 15 May 2012. The lightning flash contained nine negative return strokes, as determined from on-site ICLRT electric field and electric field derivative measurements, descriptions of which are found in *Jerauld* [2007] and *Ngin et al.* [2013]. LAPOS recorded only the first seven return strokes due to its limited recording length. The luminosity and electric field data from the ICLRT and electric field data from the Lightning Observatory in Gainesville (LOG) [*Rakov et al.*, 2012] located at a distance of 45 km from ICLRT enable the study of not only the attachment process of a first return stroke but also that process in six subsequent strokes and the comparison of those processes in first and subsequent strokes.

2. Observation and Data

The optical instrumentation is identical to that used in our most recent study of classical triggered lightning flashes at the ICLRT and is described in detail by *Wang et al.* [2013]. The anomalous lightning flash hit a 10 m tall unused, grounded, utility pole 117 m southwest of the launching facility. A cropped still camera 5 s exposure of the lightning flash is shown in Figure 1. The LAPOS field of view is annotated in Figure 1. LAPOS viewed the lightning channel from the pole top (about 10 m above ground) to a height of 85 m above the ground, as shown
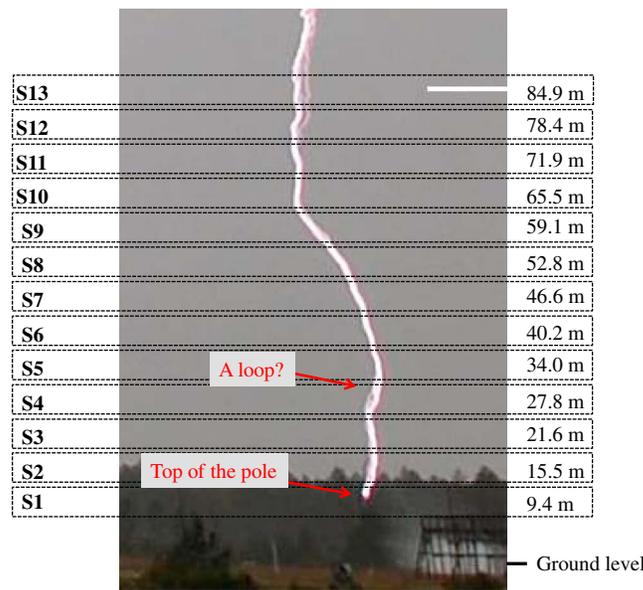
Figure 1. A still picture of the anomalous triggered lightning flash and the LAPOS view.

from S1 to S13 in Figure 1. Figure 2 presents the overall light signal of the flash. Seven return strokes and two M-components occurred during the recording period, as seen in Figure 2. As noted above, ICLRT electric field sensors recorded nine strokes. Far electric fields of the anomalous triggered flash were recorded at the Lightning Observatory in Gainesville (LOG), at a distance of 45 km from ICLRT. The LOG electric field measuring system included an elevated circular flat-plate antenna followed by an integrator and a high input impedance amplifier. The upper frequency bandwidth of the system is 10 MHz and the decay time constant is 10 ms. The record length was 2 s with 0.8 s of pretrigger and 1.2 s of posttrigger, which is long enough to record all strokes in a triggered flash. A dedicated phone line is used to transmit a trigger signal from ICLRT to LOG in the event of a lightning discharge at ICLRT. Additional details can be found in *Rakov et al.* [2012] and *Mallick et al.* [2012]. LOG electric field sensors recorded eight strokes. The National Lightning Detection Network (NLDN) reported only six return strokes. The NLDN-reported peak currents of return strokes $R1$, $R2$, $R3$, $R5$, and $R7$ in Figure 2 are 10.7 kA, 17.2 kA, 14.3 kA, 6.8 kA, and 8.1 kA, respectively. LOG electric field measurements and peak return stroke currents derived from the measured initial field peaks are presented later. One of the M-components in Figure 2 is used to calibrate the high sensitivity signals shown in the next sections, as described by *Wang et al.* [2013].

3. Results

3.1. Attachment Processes

We will first examine the luminous characteristics of the attachment processes of three leader/return stroke sequences, one being the stepped leader/first return stroke sequence, one representing dart leader/return stroke sequences, and one representing dart-stepped leader/return stroke sequences.
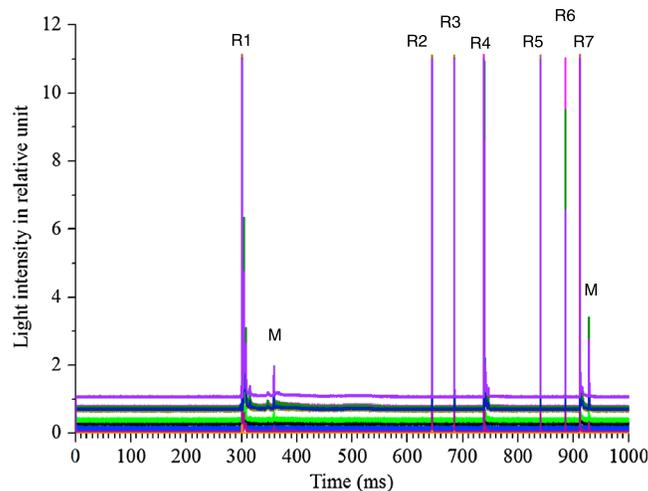

Figure 2. One second recording of the optical signal of the anomalous rocket-triggered lightning flash. Seven return strokes and two pronounced M-components occurred during the recording period.

Figure 3 shows the light signals radiated from 13 consecutive channel sections of the stepped leader/return stroke sequence, where S1–S5 signals are sampled at 100 MHz and S6–S13 are sampled at 10 MHz as described by *Wang et al.* [2013]. Each of the channel sections has a vertical height of about 4.5 m with the section central heights ranging from 9.4 m to 84.9 m above the ground level. Since the utility pole height is about 10 m, the lightning channel termination point is near the central part of S1. The signals from the lightning channel sections S1, S3, S5, S7, S9, S11, and S13 are the outputs from
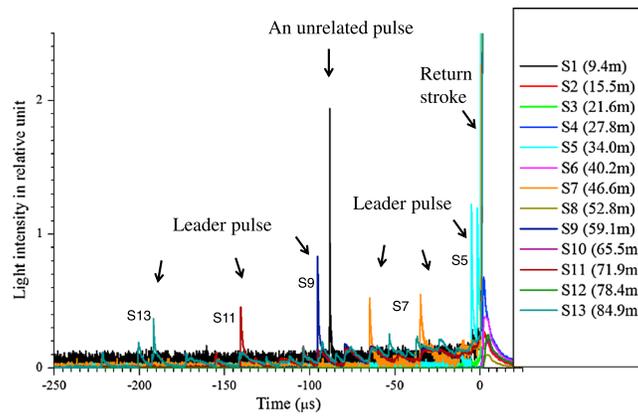
Figure 3. Light signals of the stepped leader/the first stroke sequence of the anomalous triggered lightning flash at 13 sequentially increased heights above the lightning channel termination point. Time 0 corresponds to the initiation time of the return stroke.

the high sensitivity channels of LAPOS, while the signals from S2, S4, S6, S8, S10, and S12 are the outputs from the low sensitivity channels. Time 0 in Figure 3 is subjectively chosen by comparing the features of all the waveforms and denotes the approximate initiation time of the return stroke. Light pulses can be clearly identified first on the high sensitivity channel S13, then S11, S9, S7, and S5 as shown in Figure 3. These pulses are produced by leader steps [e.g., *Chen et al.*, 1999; *Lu et al.*, 2008], and they clearly indicate that a

stepped leader is moving downward from S13 to S5. The single pulse occurring at $-88\,\mu s$ at S1 in Figure 3 is produced by a discharge at the top of a 17 m unexploded wire section connected to the rocket launcher [*Gamerota et al.*, 2013] and is used to synchronize the luminosity and the dE/dt signals shown in Figure 5.

An expanded version of the first return stroke luminous features in Figure 3 is shown in Figure 4. From the high sensitivity signals, the return stroke apparently started at S5 (34.0 m above ground) with an uncertainty of ± 10.2 m limited by the LAPOS high sensitivity channel spatial resolution, and then one return stroke wave propagated upward to S7, S9, while another wave propagated downward to S3 and S1. In these high sensitivity records, we are not able to clearly separate in time the return stroke light signals from S9, S11, and S13. This observation may indicate acceleration in the upward propagation of the return stroke as observed by *Olsen et al.* [2004]. From the low sensitivity signals, one can see that the return stroke started at S4 (27.8 m above ground) with an uncertainty of ± 10.2 m limited by the LAPOS low sensitivity channel spatial resolution, and then one wave propagated upward to S6, S8; another wave propagated downward to S2. In these low sensitivity records, similarly we are not able to clearly separate in time the return stroke light signals from S10 and S12. After combining the high and the low sensitivity signals, the return stroke was identified to initiate at S5 with a smaller uncertainty of ± 4.0 m above ground.

In response to the downward stepped leader, there should be an upward connecting leader, as observed by *Wang et al.* [2001]. However, in Figures 3 and 4, although there is some increase in the light signals at S1 and S3, we were not able to determine if these signals are caused by an upward leader or by some scattered light from the downward leader.

Figure 4. An expanded version of the light signals of the stepped leader/first stroke sequence of the anomalous triggered lightning flash at 13 sequentially increased heights above the lightning channel termination point.

In order to measure the leader speed and the return stroke speed, we need to determine their "starting points" at two different heights (or LAPOS channels). For this, we have used the so-called slope-intercept method of *Olsen et al.* [2004], as described in detail by *Wang et al.* [2013]. The estimated leader speed is 2.3×10^5 m/s, a typical value for downward propagating negative stepped leaders. The estimated return stroke upward speed from S5 to S13 is
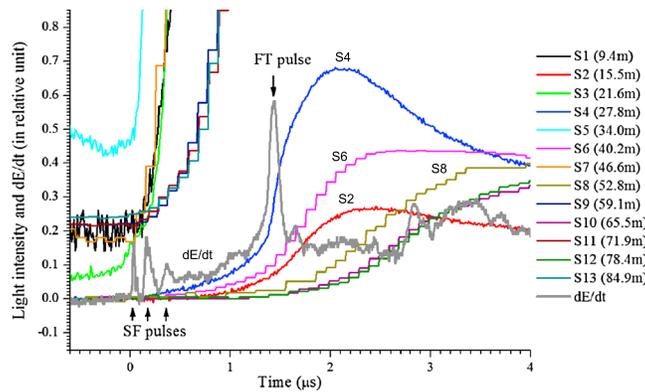
Figure 5. dE/dt slow front (SF) pulses and fast transition (FT) pulse versus LAPOS light signals for the first stroke. dE/dt and light signals are aligned with the unrelated pulse at −88 μs in Figure 3.

1.4×10^8 m/s, and the downward speed from S4 to S2 is 2.2×10^7 m/s. For a return stroke speed, the latter is apparently extremely low [e.g., *Rakov and Uman*, 2003]. Perhaps, at the instant when the return stroke occurs the corresponding upward connecting leader is still faint compared to the downward leader and the channel produced by this upward leader does not have much conductivity. Such poor conductivity may have limited the downward return stroke speed.

Electric field derivative waveforms have been previously used at the ICLRT to study the so-called slow front and fast transition of a return stroke [*Jerauld et al.*, 2007; *Howard et al.*, 2010]. For the anomalous first return stroke, both pronounced slow front (SF) and fast transition (FT) pulses are observed. In Figure 5 those SF and FT pulses recorded by a dE/dt antenna 105 m from the LAPOS location are shown along with the light signals. It is interesting to note that the first SF pulse corresponds exactly to the initiation of the return stroke at the height of S5, while the FT pulse corresponds to the beginning of a fast rise in the light signal at S4. On the other hand, a fast rise to the light signal similar to that seen at S4 did not appear either at *S2* or *S6, S8, S10,* and *S12*. Apparently due to propagation effects, the fast transition which started at S4 (more likely at S5) degraded and became unpronounced at either at *S2* or *S6, S8, S10,* and *S12*. These observations combined indicate that the slow front and fast transition are two distinctive discharge processes and both start at the return stroke initiation height.

Figures 6 and 7 present the light signals of the second return stroke and the fourth return stoke, respectively. The insets in the figures are expanded versions of the corresponding return strokes. The second stroke was preceded by a dart leader while the fourth stroke was preceded by a dart stepped leader. All subsequent strokes in the anomalous triggered lightning discharge are found to be similar to the subsequent strokes in classical rocket-triggered lightning discharges previously studied by *Wang et al.* [2013].

We have estimated the leader speed, the upward return stroke speed, the downward return stroke speed where possible, and the return stroke initiation height above the utility pole top (10 m) for all the seven leader/return stroke sequences. The results with initiation height determined from two different techniques are listed in Table 1. The first technique involves simply identifying the source of the first bright light (next to last column of Table 1) as described in third paragraph of section 3.1. In the second technique, we assume that both the leaders and the return strokes propagate constantly at their individual speeds during the attachment process, from which the return stroke initiation heights can be estimated by the time difference between the leader signal and the return stroke signal measured at S5 for strokes *R1*–*R4* and S3 for strokes *R5*–*R7*


Figure 6. Light signals of the second stroke of the anomalous triggered lightning flash at 13 sequentially increased heights above the lightning channel termination point. Time 0 corresponds to the initiation time of the return stroke. An expanded return stroke signal is shown in the inset.
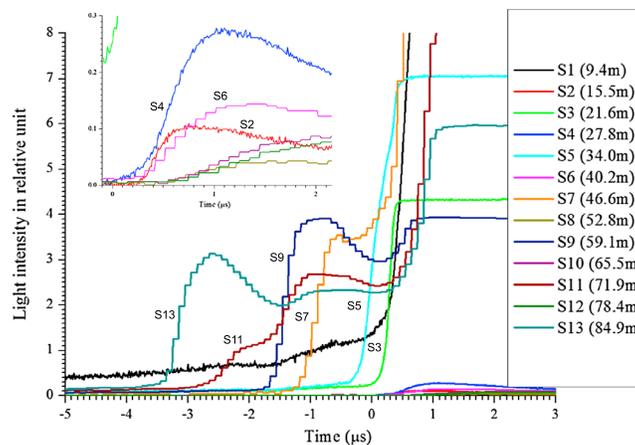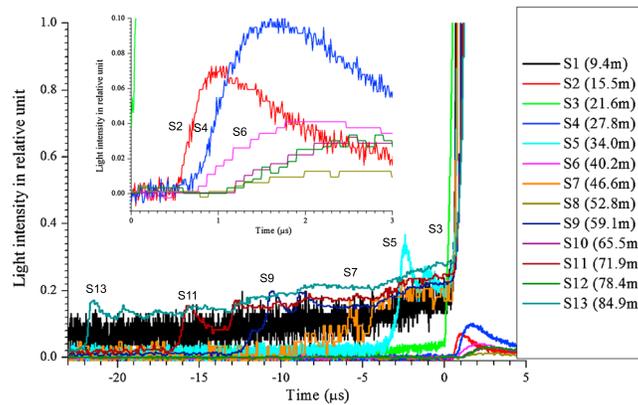
Figure 7. Light signals of the fourth stroke of the anomalous triggered lightning flash at 13 sequentially increased heights above the lightning channel termination point. Time 0 corresponds to the initiation time of the return stroke. An expanded return stroke signal is shown in the inset.

(rightmost column of Table 1). The details of this technique including the relevant uncertainty estimation have been given by *Wang et al.* [2013]. As seen in Table 1 the first return stroke initiation height is 22.7 ± 2.7 m above the top of the pole from technique 2, and in the range 24.0 ± 4.0 m from technique 1. It is interesting to note that there appears, arguably, to be a loop at the height very near the return stroke initiation height in the still photo of all strokes shown in Figure 1. Such loops have been previously observed and used to estimate the junction height of a downward leader and an upward leader [e.g., *Golde*, 1973; *Uman*, 2008]. Our result obtained with a high-speed optical system may support such conventional estimation.

3.2. Return Stroke Peak Current Versus Return Stroke Initiation Height

Using the data of classical rocket-triggered lightning, *Wang et al.* [2013] found that return strokes with larger peak current tend to initiate higher. In this section, we attempt to determine if this relationship holds true for the anomalous triggered-lightning strokes. To do so, we need information on the return stroke peak currents which could not be directly measured as was done in *Wang et al.* [2013]. As shown in the following sections, we can obtain the approximate return stroke peak currents indirectly by using three different data sets: (1) NLDN peak currents, although NLDN did not report two of the return strokes, as noted in section 2; (2) distant radiation field peaks measured at 45 km from the lightning strike point; and (3) channel bottom peak luminosities. In the following section 3.2.1, we first present the data sets (2) and (3). In section 3.2.2, we then describe the methods for estimating the peak currents and the results obtained. In section 3.2.3, we show how the return stroke initiation heights relate to the return stroke peak currents obtained using the three different data sets.

3.2.1. Return Stroke Peak Channel Bottom Luminosity and Distant Electric Fields

Figure 8 shows the luminosity waveforms of all seven return strokes at the lowest low-sensitive channel section S2, which should best reflect the electric current at the ground level among all the recorded light signals shown above, aligned in time with a common time zero. As seen in Figure 8, the first return stroke waveform rises more slowly and has a two or more times larger amplitude than that of the subsequent strokes. The zero-to-peak rise time of the first stroke is about 1.8 μs, while rise times of the subsequent strokes are shorter: 0.5 μs, 0.5 μs, 0.4 μs, 0.5 μs, 0.4 μs, and 0.4 μs, respectively. Such luminosity rise-time difference between the first return stroke and the subsequent strokes are consistent with previous findings for first and subsequent stroke electric field rise-times both from electric radiation field waveforms [e.g., *Weidman and Krider*, 1978] and electric current waveforms directly measured on tall grounded structures [e.g., *Berger et al.*, 1975].

Table 1. Summary of Various Propagation Speeds and Return Stroke Initiation Heights

Return Stroke No.	Leader Type From Luminosity Observations	Leader Speed (m/s)	Upward Return Stroke Speed (m/s)	Downward Return Stroke Speed (m/s)	Initiation Height Above Pole From First Light (m)	Return Stroke Initiation Height Above Pole From Leader Speed (m)
1	Stepped	2.3×10^5	1.4×10^8	2.2×10^7	24.0 ± 4.0	22.7 ± 2.7
2	Dart	1.8×10^7	1.4×10^8	2.1×10^8	17.8 ± 4.0	15.9 ± 2.4
3	Dart	7.6×10^6	1.1×10^8	1.7×10^8	17.8 ± 4.0	15.5 ± 2.4
4	Dart-stepped	2.7×10^6	1.2×10^8	1.1×10^8	11.6 ± 4.0	13.0 ± 5.6
5	Dart-stepped	5.3×10^6	0.8×10^8	-	11.6 ± 4.0	9.0 ± 3.1
6	Dart-stepped	0.7×10^6	1.3×10^8	-	11.6 ± 10.2	11.5 ± 2.3
7	Dart	9.4×10^6	1.1×10^8	-	11.6 ± 4.0	8.1 ± 1.1
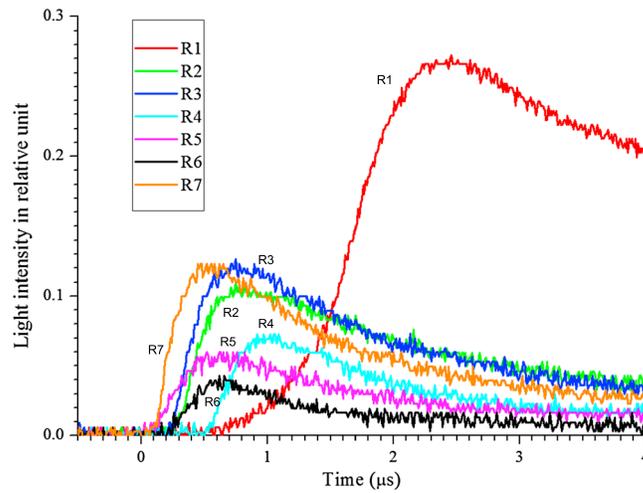
Figure 8. Channel bottom light waveforms of the seven return strokes recorded by LAPOS.

Figure 9 shows the electric fields for all strokes measured at 45 km from the lightning strike point. From these waveforms, it is seen again that the first return stroke field rises slower than that of subsequent strokes, consistent with the trend observed in luminosity waveforms.

From the waveforms shown in Figures 8 and 9, we have measured the corresponding return stroke peak luminosity in relative units and the peak radiation field at 45 km. The results are listed in Table 2.

From Table 2, it is interesting to note that although the peak luminosity of the first return stroke is significantly greater, at least 2.5 times, than for all the subsequent return strokes, the peak radiation field of the first return stroke measured at 45 km is smaller than that of the second and the third return strokes.

3.2.2. Return Stroke Peak Current Estimated From the Measured Electric Fields and From the Channel Bottom Luminosity

Mallick et al. [2012] have shown that the simple formula below relating distant radiation field E_r and peak current I, corresponding to the transmission line return stroke model [*Uman and McLain*, 1969; *Uman et al.*, 1975], works well for subsequent strokes triggered at the ICLRT when the return stroke speed v is chosen to be between 1/3 and 1/2 the speed of light c

$$I = \frac{2\pi\varepsilon_0 c^2 r}{v} E_r \qquad (1)$$

with r being the distance from measurement to lightning striking point and c the speed of light.

The NLDN in effect uses some version of the above equation, with fields corrected for propagation and attenuation of the radiation field peaks caused by the finite conductivity ground plane, to calculate stroke peak current [*Jerauld et al.*, 2005; *Nag et al.*, 2011, *Mallick et al.*, 2012].

With formula (1), the return stroke peak radiation fields in the third column of Table 2 measured at 45 km are converted into peak return stroke currents listed in the third column of Table 3.

According to the measurements made by *Wang et al.* [2005] on triggered lightning strokes, equivalent to subsequent strokes in natural lightning, the channel bottom peak light of a subsequent return stroke is proportional to its peak current. No similar information for first strokes is available. However, if we assume
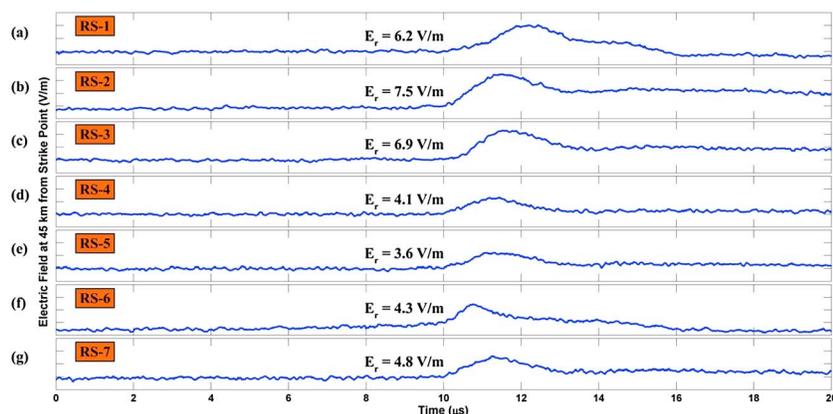

Figure 9. (a–g) Electric field at 45 km from the strike point for the first seven return strokes of the anomalous triggered lightning flash. Each subplot has the same vertical scale with each tick representing 3 V/m.

Table 2. Return Stroke Intensities in Various Measurements

Return Stroke No.	Channel Bottom Light Intensity (in Relative Unit)	45 km Electric Radiation Field Peak (V/m)
1	0.27	6.2
2	0.11	7.5
3	0.12	6.9
4	0.07	4.1
5	0.06	3.6
6	0.04	4.3
7	0.12	4.8

that subsequent-stroke relationship is also applicable to the first stroke, that is, it is applicable to all strokes in the flash, we can convert the peak luminosity shown in the second column of Table 2 into peak return stroke current through the following approach.

First, as several NLDN evaluation experiments employing rocket-triggered lightning data have shown that NLDN average subsequent stroke peak currents are very similar to the directly measured average peak current [e.g., *Nag et al.*, 2011], by averaging the NLDN peak currents of the subsequent return strokes, $R2$, $R3$, $R5$, and $R7$, we get an adequate average peak return stroke current for subsequent strokes. Then, by correlating the average NLDN peak current and the average peak luminosity of the corresponding subsequent strokes, we can derive a conversion factor between the current and the peak luminosity, which is 113 kA/per relative unit light intensity. Finally, by using this conversion factor, we convert the peak light intensities in Table 2 into peak return stroke currents as given in the fourth column of Table 3.

3.2.3. Return Stroke Initiation Height Versus Peak Currents

Figure 10 gives the scatterplots of the return stroke initiation height versus the return stroke peak currents obtained from the three different data sets, (a) NLDN peak current, (b) peak current estimated from 45 km radiation field, and (c) peak current estimated from channel bottom luminosity. For comparison, the relationship between the return stroke initiation height and the peak current derived for subsequent strokes in classical rocket-triggered lightning [*Wang et al.*, 2013] has been included. For the subsequent return strokes, all three data sets show a trend for a return stroke with a larger current to be initiated higher, which is similar to what *Wang et al.* [2013] found for classical rocket-triggered-lightning return strokes. However, for the first return stroke, the scatterplot based on the luminosity peak return stroke data set shows that the first stroke follows the same trend as subsequent strokes, as seen in Figure 10c, while the NLDN and 45 km radiation field data sets show that the first stroke deviates significantly from the trend expected for subsequent strokes, as seen in Figures 10a and 10b. The first return stroke in Figures 10a and 10b initiates much higher than expected for subsequent strokes with the same peak current.

4. Discussion

The initiation of the first return stroke was found to occur at a height of 22.7 ± 2.7 m above the top of the utility pole and was associated with three slow front dE/dt pulses and a fast transition dE/dt pulse. The slow front and fast transition dE/dt pulses of the first return stroke occurred in time coincidence with the slow front luminosity marking the beginning of the return stroke and the fast transition luminosity marking the beginning of the fast rise discharge process of the return stroke, respectively. Historically, the slow front has often been attributed to the presence of the associated upward connecting leader [e.g., *Weidman and Krider*, 1978; *Rakov and Uman*, 2003]. *Jerauld et al.* [2007] proposed a model in which both the slow front and fast transition currents are generated at the junction point of the upward and downward leaders and propagate away from that point. A similar model, but extended to include reflection from ground, was used by *Nag et al.* [2012]. Our results provided direct evidence for the model proposed by *Jerauld et al.* [2007].

Table 3. Comparison of Estimated Peak Current From NLDN, Radiation Field at 45 km, and Channel Bottom Luminosity

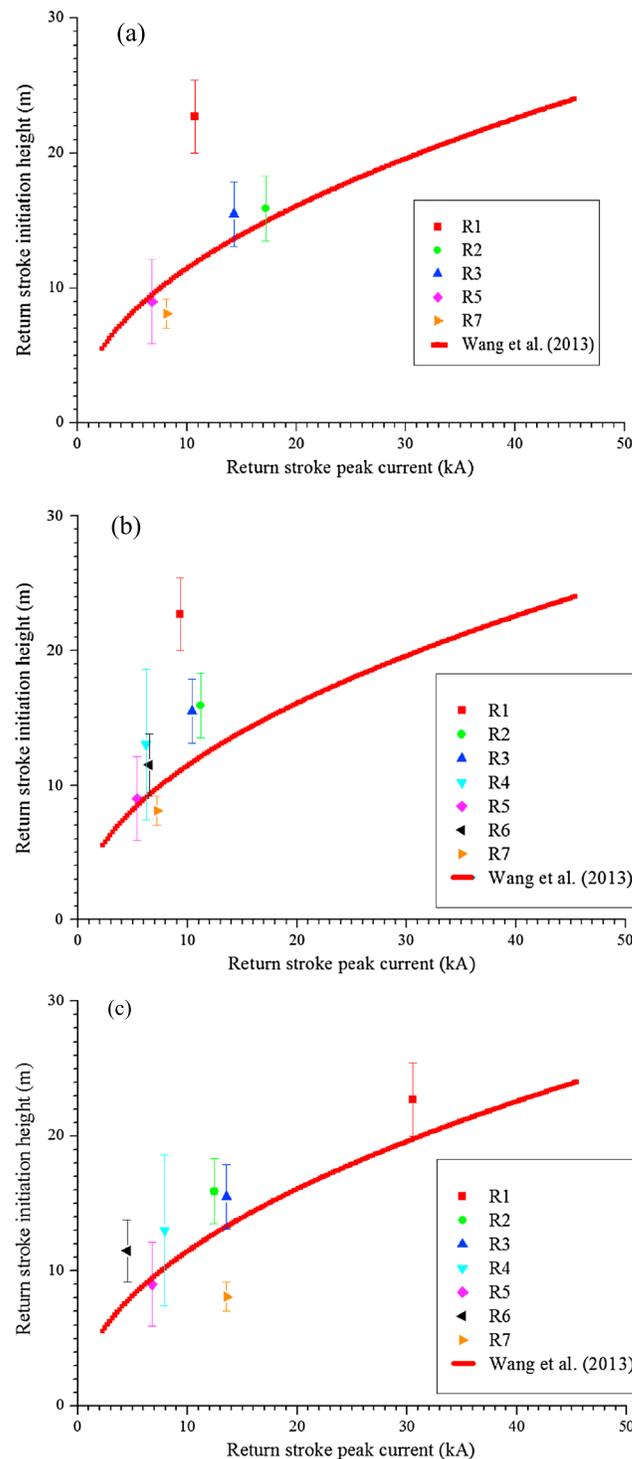| Return Stroke No.	NLDN-Estimated Peak Current (kA)	45 km E_r-Estimated Peak (Assuming $v = c/2$) Current (kA)	Estimated Peak Current From Peak Luminosity (kA)
1	−10.7	−9.3	−30.5
2	−17.2	−11.2	−12.4
3	−14.3	−10.4	−13.6
4	N/A	−6.2	−7.9
5	−6.8	−5.4	−6.8
6	N/A	−6.5	−4.5
7	−8.1	−7.2	−13.6

Figure 10. A scatterplot of return stroke initiation height versus return stroke peak current: (a) NLDN peak current, (b) peak current estimated from distant radiation field, and (c) peak current estimated from channel bottom luminosity. The red line is adapted from *Wang et al.* [2013] for classical rocket-triggered strokes.

Using a dE/dt time-of-arrival technique, *Howard et al.* [2010] have obtained 3-D source locations of slow front (SF) and fast transition (FT) dE/dt pulses for three natural first strokes. They found that both the SF and FT pulses originated from the same general region. Our results are consistent with their results. The SF pulse marks the initiation of the return stroke while the FT pulse marks the beginning of the sharp rise in luminosity, and thereafter in current. Clearly, the slow front and the fast transition processes are two distinctive processes. As shown in Figure 5, three SF dE/dt pulses occurred during the initial stage of the first return stroke, only the first SF dE/dt pulse corresponds to the beginning of the first return stroke. Similar multiple SF dE/dt pulses have been reported by *Howard et al.* [2010]. They speculated that multiple SF dE/dt pulses are caused by multiple connections of downward and upward leaders via different branches. Indeed, as seen in Figure 1, there are at least two branches at the height just below the return stroke initiation height of 33 m above ground. Thus, we agree with their speculation.

The scatterplots of return stroke initiation height versus return stroke peak current shown in Figure 10 exhibited two different trends for the first return stroke. When the peak currents derived from channel bottom luminosity are used, the first return stroke and the subsequent return strokes appear to share a similar dependence of initiation height on peak current. When the peak currents estimated from measured electric radiation fields or NLDN peak currents are used, the first return stroke and the subsequent return strokes appear to have different initiation heights for the same peak current, with the first return stroke being initiated higher. It is thought that there is a linear correlation between peak current and charge on the downward leader [e.g., *Cooray et al.*, 2007], and thus, the leader electrostatic field change at the ground. In the case of first strokes, the corresponding upward connecting leader is induced in virgin air, while in the case of the subsequent strokes, the upward leader is induced in a preconditioned channel. Thus, if the first and the subsequent return strokes were the same, the upward leaders of the subsequent strokes should,
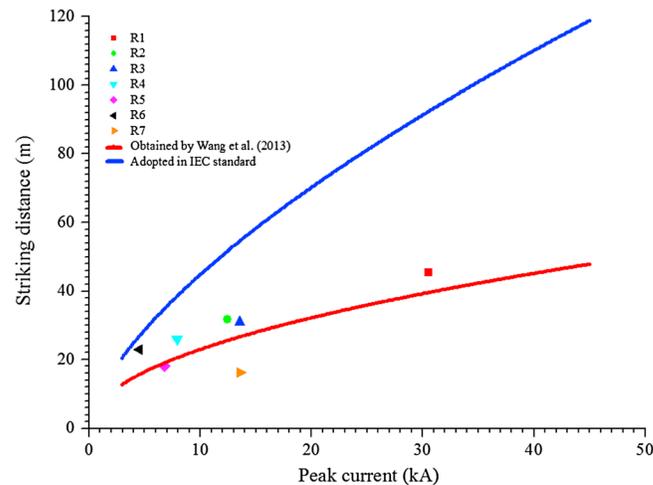
Figure 11. Striking distance, 2 times the initiation height in Figure 10, versus return stroke peak current derived from luminosity. The red line is adapted from *Wang et al*. [2013] for classical rocket-triggered strokes. The blue curve was adapted from *IEC standard* [2010].

arguably, be initiated earlier and propagate faster, and this would, again arguably, result in a higher return stroke initiation height, opposite to those trends obtained when the peak currents via measured electric fields are used. Note, however, that conditions for initiation of upward connecting leaders in subsequent stokes are presently unclear. Using data from two electric field antennas, located 110 m northeast and 280 m due east from the strike point of the anomalous lightning in the present study, *Gamerota et al.* [2013] estimated the charge density along the channel bottom (with a length close to 282 m) of the stepped leader to be 1.7 to 3.3×10^{-3} C/m, which is similar or slightly larger than the channel bottom charge density of a

stepped leader calculated by *Cooray et al.* [2007] assuming that its return stoke peak current is 30 kA. Further, according to the peak currents measured by *Berger et al.* [1975], the peak currents of the first return stroke is generally 2.5 times larger than the subsequent return strokes. As seen in Table 3, only the peak currents estimated via the channel bottom luminosity is consistent with the results given by *Berger et al.* [1975]. This may appear to imply that first-stroke peak currents inferred from radiation field peaks are underestimates. However, the ratio of radiation field peaks for first and subsequent strokes from measurements in different countries is about 2 [*Nag et al.*, 2008], which is not much different from the corresponding ratio for currents (2.5). Taking all these factors into consideration, we suggest that the peak currents estimated via the luminosity, and thereafter the corresponding return stroke initiation height versus peak current shown in Figure 10c are likely to be true, but further research is clearly needed. There may be reasons other than a larger first stroke current, although they are not obvious, for the fact that the ratio of the first stroke luminosity to subsequent stroke luminosity is much greater than their ratio for the radiation field peaks in this particular flash. Among these reasons could be the presence of a larger corona sheath surrounding the first stroke or the fact that the first stroke leader and the first stroke breakdown process are occurring in virgin air and involve multiple connecting branches.

According to high-speed videos showing the simultaneous approach of a downward leader and its connecting upward leader, the two leaders usually have similar progression speeds [*Lu et al.*, 2010]. The only observed propagation speed of an upward connecting leader in a rocket-triggered lightning discharges is also similar to that of its corresponding downward dart leader [*Wang et al.*, 1999]. Assuming that this is the case for all seven strokes studied here, doubling the return stroke initiation heights above the lightning terminus point will result in striking distances, an assumption made in a previous study by *Wang et al.* [2013]. Figure 11 shows the scatterplot of the striking distance versus the peak current derived from luminosity. As a comparison, the striking distance versus peak current curve used in IEC (International Electrotechnical Commission) standard 62305-1:2010 is included in Figure 11. Our estimated striking distance is significantly smaller than the IEC recommended striking distance, especially for strokes with larger peak currents.

Among the four return strokes which allowed us to measure their downward return stroke speeds, only the first return stroke had an extremely low downward speed, 2.2×10^7 m/s, about 5 to 10 times lower than the remaining three strokes. A lower propagating return stroke wave will radiate smaller electromagnetic waves [e.g., *Miyazaki and Ishii*, 2006]. This may be one factor which has led into the underestimation (which is still in need of confirmation as discussed above) of the NLDN and LOG radiation field-derived first return stroke peak current.

5. Summary

We have documented the lightning attachment process of an anomalous rocket-triggered lightning that terminated on a 10 m high unused, grounded utility pole. The initiation of the first return stroke was found to

occur at a height of 23 ± 3 m above the top of the utility pole and was associated with three slow front dE/dt pulses. A time of 1.5 μs later, a fast rise in luminosity at 20 ± 2 m was associated with a fast transition dE/dt pulse. The first return stroke propagated bidirectionally from its initiation height, as did subsequent return strokes from their initiation heights of 8 ± 1 m to 16 ± 2 m above the top of the utility pole. The initial upward speed of the first return stroke was 1.4×10^8 m/s, while its initial downward speed was 2.2×10^7 m/s. The channel bottom luminosity of the first return stroke rose more slowly to a two or more times larger amplitude than that of the subsequent stroke luminosities. In contrast, the NLDN-derived first-return-stroke peak current is smaller than that of the second and the third strokes, and our electric field records at 45 km show a similar behavior for the initial field peaks of the first and subsequent strokes. Using the luminosity and the distant electric field, respectively, we have estimated the return stroke peak currents and found that the luminosity-estimated first return stroke current is more than twice larger than those reported by the NLDN or based on distant electric field. The return stroke initiation height versus current of the anomalous lightning appears to be consistent with classical rocket-triggered strokes only when the luminosity-estimated currents are used.

References

Berger, K., P. B. Anderson, and H. Kroninger (1975), Parameters of lightning flashes, *Electra*, *80*, 223–237.

Chen, M., N. Takagi, T. Watanabe, D. Wang, Z.-I. Kawasaki, and X. Liu (1999), Spatial and temporal properties of optical radiation produced by stepped leader, *J. Geophys. Res.*, *104*, 27,573–27,584.

Cooray, V., V. Rakov, and N. Theethayi (2007), The lightning striking distance—Revisited, *J. Electrostat.*, *65*, 296–306.

Gamerota, W. R., M. A. Uman, J. D. Hill, J. Pilkey, T. Ngin, D. M. Jordan, and C. T. Mata (2013), An "anomalous" triggered lightning flash in Florida, *J. Geophys. Res. Atmospheres*, *118*, 3402–3414, doi:10.1002/jgrd.50261.

Golde, R. H. (1973), *Lightning Protection*, Edward Arnold, Ltd., London.

Howard, J., M. A. Uman, C. Biagi, D. Hill, J. Jerauld, V. A. Rakov, J. Dwyer, Z. Saleh, and H. Rassoul (2010), RF and X-ray source locations during the lightning attachment process, *J. Geophys. Res.*, *115*, D06204, doi:10.1029/2009JD012055.

IEC standard 62305-1 (2010), Protection against lightning. Part 1: General principles. Geneva: International Electrotechnical Commission.

Jerauld, J. E. (2007), Properties of natural cloud-to-ground lightning inferred from multiple-station measurements of close electric and magnetic fields and field derivatives, PhD dissertation, Univ. of Fla., Gainesville. [Available at http://purl.fcla.edu/fcla/etd/UFE0021279.]

Jerauld, J., V. A. Rakov, M. A. Uman, K. J. Rambo, D. M. Jordan, K. L. Cummins, and J. A. Cramer (2005), An evaluation of the performance characteristics of the U.S. National Lightning Detection Network in Florida using rocket-triggered lightning, *J. Geophys. Res.*, *110*, D19106, doi:10.1029/2005JD005924.

Jerauld, J., M. A. Uman, V. A. Rakov, K. J. Rambo, and G. H. Schnetzer (2007), Insights into the ground attachment process of natural lightning gained from an unusual triggered-lightning stroke, *J. Geophys. Res.*, *112*, D13113, doi:10.1029/2006JD007682.

Lu, W., D. Wang, N. Takagi, V. Rakov, M. Uman, and M. Miki (2008), Characteristics of the optical pulses associated with a downward branched stepped leader, *J. Geophys. Res.*, *113*, D21206, doi:10.1029/2008JD010231.

Lu, W., Y. Zhang, L. Chen, E. Zhou, D. Zheng, Y. Zhang, and D. Wang (2010), Attachment process of two natural downward lightning flashes striking on high structures, Proceedings of 30th International Conference on Lightning Protection, Paper number 1260.

Mallick, S., et al. (2012), On remote measurements of lightning return stroke peak currents, *Atmos. Res.*, doi:10.1016/j.atmosres.2012.08.008.

Miyazaki, S., and M. Ishii (2006), Reproduction of time derivative of electromagnetic field associated with rocket-triggered lightning in submicrosecond range, *J. Geophys. Res.*, *111*, D22203, doi:10.1029/2005JD006471.

Nag, A., V. A. Rakov, W. Schulz, M. M. F. Saba, R. Thottappillil, C. J. Biagi, A. O. Filho, A. Kafri, N. Theethayi, and T. Gotschl (2008), First versus subsequent return-stroke current and field peaks in negative cloud-to-ground lightning discharges, *J. Geophys. Res.*, *113*, D19112, doi:10.1029/2007JD009729.

Nag, A., et al. (2011), Evaluation of U.S. National Lightning Detection Network performance characteristics using rocket-triggered lightning data acquired in 2004–2009, *J. Geophys. Res.*, *116*, D02123, doi:10.1029/2010JD014929.

Nag, A., V. A. Rakov, D. Tsalikis, J. S. Howard, C. J. Biagi, J. D. Hill, M. A. Uman, and D. M. Jordan (2012), Characteristics of the initial rising portion of near and far lightning return stroke electric field waveforms, *Atmos. Res.*, *117*, 71–77.

Ngin, T., M. A. Uman, J. D. Hill, J. Pilkey, W. R. Gamerota, D. M. Jordan, and R. C. Olsen III (2013), Measurement and analysis of ground-level electric fields and wire-base current during the rocket-and-wire lightning triggering process, *J. Geophys. Res. Atmos.*, *118*, 10,041–10,055, doi:10.1002/jgrd.50774.

Olsen, R. C., III, D. M. Jordan, V. A. Rakov, M. A. Uman, and N. Grimes (2004), Observed one-dimensional return stroke propagation speeds in the bottom 170 m of rocket-triggered lightning channel, *Geophys. Res. Lett.*, *31*, L16107, doi:10.1029/2004GL020187.

Rakov, V. A., and M. A. Uman (2003), *Physics and Effects*, Cambridge Univ. Press, Cambridge, U. K.

Rakov V. A., S. Mallick, and A. Nag (2012), Lightning observatory in Gainesville (LOG), Florida: A review of recent results, Proc. of 2012 International Conference on Lightning Protection (ICLP), Vienna, Austria.

Uman, M. A., and D. K. McLain (1969), Magnetic field of lightning return stroke, *J. Geophys. Res.*, *24*(28), 6899–6910.

Uman, M. A., D. K. McLain, and E. P. Krider (1975), The electromagnetic radiation from a finite antenna, *Am. Jour. Phys.*, *43*, 33–38.

Uman, M. A. (2008), The Art and Science of Lightning Protection, pp. 50–77, 233–234, Cambridge Univ. Press, Cambridge, U. K.

Wang, D., V. A. Rakov, M. A. Uman, N. Takagi, T. Watanabe, D. E. Crawford, K. J. Rambo, G. H. Schnetzer, R. J. Fisher, and Z.-I. Kawasaki (1999), Attachment process in rocket-triggered lightning strokes, *J. Geophys. Res.*, *104*(D2), 2143–2150.

Wang, D., M. Chen, N. Takagi, and T. Watanabe (2001), Correlated submicrosecond-field and high-speed image of the natural lightning attachment process, in Proc. Int. Conf. Lightning and Static Elec. (ICOLSE), Society of Automotive Engineers (SAE), Seattle, Washington.

Wang, D., N. Takagi, T. Watanabe, V. A. Rakov, M. A. Uman, K. J. Rambo, and M. V. Stapleton (2005), A comparison of channel-base currents and optical signals for rocket-triggered lightning strokes, *Atmos. Res.*, *76*(1–4), 412–422.

Wang, D., T. Watanabe, and N. Takagi (2011), A high speed optical imaging system for studying lightning attachment process, Proc. of 7th Asia-Pacific Lightning Conference, Chengdu, China.

Wang, D., N. Takagi, W. R. Gamerota, M. A. Uman, J. D. Hill, and D. M. Jordan (2013), Initiation processes of return strokes in rocket-triggered lightning, *J. Geophys. Res.Atmos.*, *118*, 9880–9888, doi:10.1002/jgrd.50766.

Weidman, C. D., and E. P. Krider (1978), The fine structure of lightning return stroke wave forms, *J. Geophys. Res.*, *83*, 6239–6247.